J Therm Anal Calorim (2010) 101:371–377
DOI 10.1007/s10973-009-0618-y

Heat capacity and thermal expansion coefficient of rare earth uranates RE_6UO_{12} (RE = Nd, Gd and Eu)

R. Venkata Krishnan · Hrudananda Jena · K. V. Govindan Kutty · K. Nagarajan

Received: 16 June 2009 / Accepted: 18 November 2009 / Published online: 28 November 2009

Abstract Rare earth uranates Nd_6UO_{12}, Gd_6UO_{12} and Eu_6UO_{12} were prepared by combustion synthesis and characterized by XRD. Single-phase rhombohedral structure was observed for all the above compounds. Heat capacity measurements were carried out on Nd_6UO_{12} and Gd_6UO_{12} with differential scanning calorimetry in the temperature range 298–800 K. Enthalpy, entropy and Gibbs energy functions were computed. Heat capacity values of Nd_6UO_{12} and Gd_6UO_{12} at 298 K are 436 and 400 J K^{-1} mol^{-1}, respectively. Thermal expansion characteristics were studied using high temperature X-ray diffraction (HTXRD) in the temperature range 298–873 K. The coefficients of thermal expansion measured for Eu_6UO_{12} are 10.5×10^{-6} and 7.3×10^{-6} K^{-1} along *a*- and *c*-axis, respectively. Similarly, the coefficients of thermal expansion of Gd_6UO_{12} along *a*-axis are 10.0×10^{-6} K^{-1} and along *c*-axis is 9.7×10^{-6} K^{-1}.

Keywords Heat capacity · Rare earths · Uranates · Rare earth uranates · Thermal expansion

Introduction

RE_6UO_{12} (RE = rare earth) type of compounds are known to exist is RE–U–O system [1, 2] with rhombohedral structure [3–5]. Though RE_6UO_{12} compounds are not formed under normal reactor operation conditions, they might be formed under transient conditions and therefore thermophysical properties such as heat capacity and thermal expansion of these compounds are of interest. Thermal expansion of RE_6UO_{12} (RE = La, Nd and Sm,) were measured by by Jena et al. [5, 6] and thermal diffusivity of RE_6UO_{12} (RE = La, Gd, Dy) by Krishnaiah et al. [7]. Differential scanning calorimetry is widely used to measure heat capacity of variety of compounds such as ceramics, organic materials, polymers, ionic liquids, etc., [8–17]. Heat capacity of RE_6UO_{12} (RE = La, Sm and Eu) had been measured by DSC in our previous study [18]. In the present study heat capacity of Nd_6UO_{12} and Gd_6UO_{12} were measured by DSC and thermal expansion of Gd_6UO_{12} and Eu_6UO_{12} by HTXRD.

Experimental

Sample preparation

UO_2 of nuclear grade purity supplied by Nuclear Fuel Complex, Hyderabad, India, and RE_2O_3 (RE = Nd, Gd and Eu) of 99.9% purity supplied by M/s. Indian Rare Earths were used for preparing the samples. RE_6UO_{12} compounds were prepared by combustion synthesis, as explained in our previous paper [18]. Stiochiometric ratio of oxidant to fuel was used for the preparation. The sample pellets obtained were heated at 1,473 K in air for 8 h. As the samples were heated in air, the RE_6UO_{12} compounds prepared are expected to be stoichiometric [5]. Since citric acid was used as the fuel, the samples were analyzed for carbon impurity by using carbon analyzer of M/s. Eltra, Germany (ELTRACS 800). All the samples were found to contain <100 ppm of carbon. The sample pellets were then ground and X-ray diffraction analysis was performed on all the above mentioned samples, using Siemens D500 powder

R. Venkata Krishnan · H. Jena · K. V. Govindan Kutty · K. Nagarajan (✉)
Head, Pyrochemical Processing Studies Section, Fuel Chemistry Division, Chemistry Group, Indira Gandhi Centre for Atomic Research, Kalpakkam 603 102, Tamil Nadu, India
e-mail: knag@igcar.gov.in

diffractometer using CuKα radiation monochromatized with curved graphite crystal monochromator placed in front of the NaI(Tl) scintillation detector. The scans were made in the range of $10° \leq 2\theta \leq 80°$. The X-ray diffraction patterns of Nd_6UO_{12}, Gd_6UO_{12} and Eu_6UO_{12} are shown in Fig. 1, which are in good agreement with the reported literature patterns (JCPDS Card No.190830, JCPDS Card No. 801372, JCPDS Card No. 201335). The computed lattice parameter values of RE_6UO_{12} listed in Table 1 are in good agreement with the values reported in the literature [3, 6] (JCPDS Card No. 201335). The lattice parameter values also suggest that the RE_6UO_{12} compounds formed are stiochiometric. For DSC measurements, the powders of these samples were compacted into pellets of 5 mm in diameter and sintered at 1,673 K in air for 8 h.

Heat capacity measurements

A heat flux type differential scanning calorimeter (model number DSC821e/700 of M/s. Mettler Toledo GmbH, Switzerland) was used in this study. Pellet samples were hermetically sealed in 40 μL Al-pans and a pinhole was made on the lid. High purity argon was used as the purge gas at a flow rate of 50 mL min^{-1} and a heating rate of 10 K min^{-1} was employed in DSC measurements in the temperature range 298–800 K. A thin disc of sapphire was used as the heat capacity standard. A three segment-heating programme was used. The first segment lasting for 5 min was an isothermal one at the initial temperature; the second segment was a dynamic one with a heating rate of 10 K min^{-1} and the final segment lasting for 5 min was another isothermal one at the final temperature. The "Classical" three step procedure of three runs was used for measuring heat capacity. The first run was a blank run with empty pans on both the sample and the reference sides of the calorimeter. The blank run was for the correction of any asymmetry between the two pans. The second run was the calibration run where the calibration material, a disc of sapphire, was placed on the sample pan whereas the pan on the reference side was kept empty. The third run was the sample run where the sample in the form of pellet was placed on the sample pan with empty pan on the reference side. These three runs were repeated for each measurement of heat capacity. Temperature, heat and heat rate calibrations of the DSC were carried out, as explained in our earlier study [19, 20].

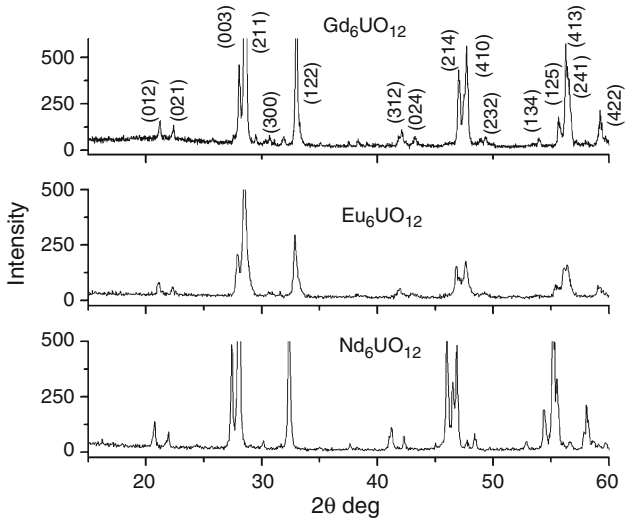

Fig. 1 Room temperature XRD patterns of RE_6UO_{12}

Thermal expansion measurements by HTXRD

HTXRD measurements were carried out by using the HTK-16 module of Philips X'Pert Pro MPD system. The powder samples were mixed with Pt powder (1:5 = Pt: Re_6UO_{12} wt. ratio) as internal standard for temperature correction. The fine powders were mounted on the tantalum strip (sample carrier) that was resistively heated at programmed heating rates. The sample temperature was monitored with a thermocouple spot- welded to the rear side of the sample carrier strip. All measurements were carried out in a

Table 1 Crystal data for the RE_6UO_{12} compounds measured by XRD

Crystal data at 298 K		Compound					
		Space group-$R\bar{3}$					
		Nd_6UO_{12}		Gd_6UO_{12}		Eu_6UO_{12}	
		This study	Literature values	This study	Literature values	This study	Literature values
Hexagonal parameters	a (Å)	10.254 (1)	10.254 [12]	10.098 (2)	10.070 [11] 10.077 [17]	10.140 (4)	10.126 [6, 12]
	c (Å)	9.748 (1)	9.748 [12]	9.554 (2)	9.529 [11] 9.526 [17]	9.569 (3)	9.601 [6, 12]
Rhombohedral parameters	a_R (Å)	6.754 (3)	–	6.643 (2)	6.6285 [17]	6.649 (4)	6.665 [6, 12]
	α(deg)	98.79	–	98.89	98.94 [17]	98.95	98.87 [6, 12]

vacuum of about 10^{-5} Torr. The XRD patterns were recorded in step scan mode with the step size of 0.02° s^{-1}. The XRD patterns of the samples were recorded at room temperatures, and then the temperature was increased to 873 K in steps of 100 K. The lattice parameters were obtained from the XRD data at each temperature. The lattice parameters, l, were fitted against temperature (in Kelvin) to the polynomial expression: $l = x + yT + zT^2$. The average axial expansion coefficient, α_l, between the temperatures, T_1 *and* T_2, was calculated by the equation, $\alpha_l = (l_2 - l_1)/(l_1(T_2 - T_1))$, where l_1 and l_2 are the lattice parameters at temperatures T_1 *and* T_2, respectively. The cell volume for this hexagonal system was computed by the expression $v = \sqrt{3}/2(a^2c)$ and the percentage variation in unit cell volume was computed by the expression $((v_T - v_{298})/v_{298}) \times 100$.

Results

Heat capacity of Nd_6UO_{12} and Gd_6UO_{12}

Heat capacity data of sapphire given by National Institute of Standards and Technology, USA (NIST) were used for computing the heat capacities of the samples. Heat capacity of Nd_6UO_{12} and Gd_6UO_{12} measured by DSC and given in Tables 2 and 3, respectively, are the mean of eight measurements. The error in the heat capacity values by our DSC measurements had been earlier determined to be ±3% by measurements on ThO_2 samples [21]. However, the relative standard deviations among the present measurements are in the range of 1–3%. Hence the uncertainty in the measured heat capacity values has been estimated to be ±3%. The measured heat capacity of Nd_6UO_{12} and Gd_6UO_{12} were least squares fitted to obtain the following polynomial in temperature.

$$C_{p,m}(Nd_6UO_{12})\left(JK^{-1}\ mol.^{-1}\right) = 702.196 - 1.3175(T/K) - 5.011332 \times 10^6\,(K/T)^2 + 2.42 \times 10^{-3}(T/K)^2 - 1.3314 \times 10^{-6}\,(T/K)^3 \times (298 - 800K) \quad (1)$$

$$C_{p,m}(Gd_6UO_{12})\left(JK^{-1}\ mol.^{-1}\right) = 500.68 + 7.07 \times 10^{-3}\,(T/K) - 9.161807 \times 10^6\,(K/T)^2 (298 - 800K) \quad (2)$$

The standard errors of the fit equations 1 and 2 are 2.8 and 2.5 J K^{-1} mol^{-1}, respectively. The measured heat capacity of Nd_6UO_{12}, and Gd_6UO_{12} along with the fit values are shown in Figs. 2 and 3, respectively. The heat capacity of Nd_6UO_{12} and Gd_6UO_{12} computed by Neumann–Kopp's law using the heat capacity data of UO_3 [22], Nd_2O_3[23] and Gd_2O_3 [23] are also shown in Figs. 2 and 3, respectively. The heat capacity data of

Table 2 Thermodynamic functions of Nd_6UO_{12}

T/K	$C_{p,m}$/J K^{-1} mol^{-1}		$H_T^0 - H_{298}^0$/J mol^{-1}	S_T^0/J K^{-1} mol^{-1}	$G_T^0 - H_{298}^0$ /*T*/J K^{-1} mol^{-1}
	Measured	Fit			
298	436	433	0	574	−574
300	436	433	866	578	−575
400	448	446	44,820	729	−617
500	458	462	90,173	841	−661
600	489	481	137,335	933	−704
700	497	499	186,395	1,013	−746
800	512	508	236,821	1,082	−786

Table 3 Thermodynamic functions of Gd_6UO_{12}

T/K	$C_{p,m}$/J K^{-1} mol^{-1}			$H_T^0 - H_{298}^0$/J mol^{-1}	S_T^0/J K^{-1} mol^{-1}	$G_T^0 - H_{298}^0$ /*T*/J K^{-1} mol^{-1}
	Measured	Fit	Sahu et al. [17]			
298	400	400	386	0	551	−551
300	401	401	386	801	553	−551
400	446	446	416	43,481	676	−567
500	471	468	439	89,286	778	−599
600	480	479	454	136,689	864	−637
700	483	487	459	185,036	939	−675
800	499	492	456	233,998	1,004	−712

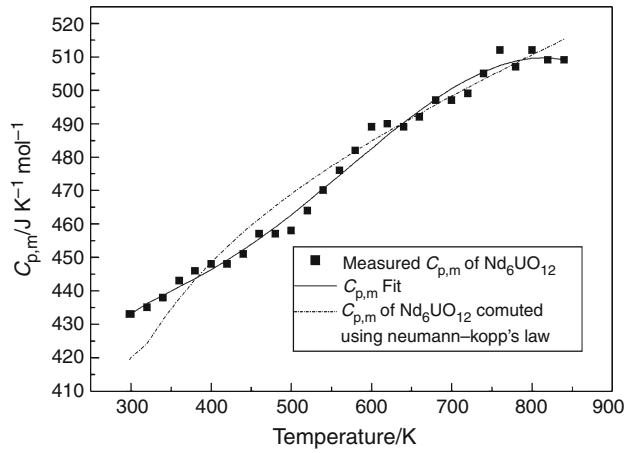

Fig. 2 Heat capacity data of Nd_6UO_{12}

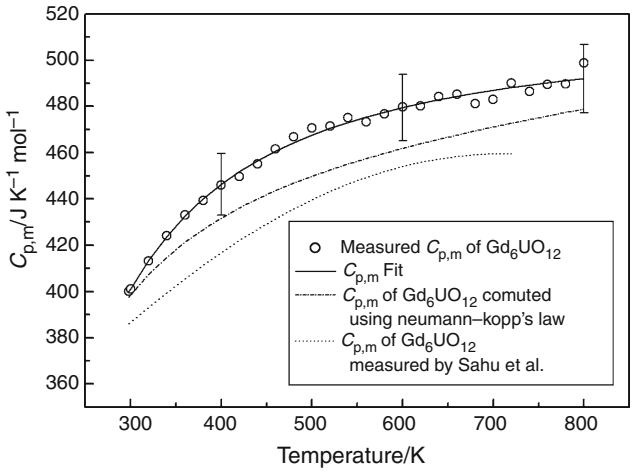

Fig. 3 Heat capacity data of Gd_6UO_{12}

respective component oxides used for the computation are given below

$$C_{p,m}(UO_3)\left(J\ K^{-1}\ mol^{-1}\right) = 90.374 + 11.046 \times 10^{-3}\,(T/K) - 1.109 \times 10^{6}(K/T)^2 \quad (3)$$

$$C_{p,m}(Nd_2O_3)\left(J\ K^{-1}\ mol^{-1}\right) = 115.52 + 29.999 \times 10^{-3}(T/K) - 1.167 \times 10^{6}(K/T)^2 \quad (4)$$

$$C_{p,m}(Gd_2O_3)\left(J\ K^{-1}\ mol^{-1}\right) = 119.206 + 12.945 \times 10^{-3}(T/K) - 1.561 \times 10^{6}(K/T)^2 \quad (5)$$

As can be seen in the figure the present data are in good agreement within ±3% with that computed using Neumann–Kopp's law using the heat capacity of their respective component oxides. However, the heat capacity data of Gd_6UO_{12} measured by Sahu et al. [24] are about 3–6% less than the present data. From the heat capacity data, other thermodynamic functions such as enthalpy, entropy and Gibbs energy functions of Nd_6UO_{12} and Gd_6UO_{12} were computed and are given in Tables 2 and 3, respectively. The S^0_{298} values of Nd_6UO_{12} and Gd_6UO_{12} required for the computation of entropies were estimated by using S^0_{298} of their respective component oxides (Nd_2O_3, Gd_2O_3 and UO_3) from the literature [22, 23] as explained below. The estimated value of S^0_{298} for Nd_6UO_{12} and Gd_6UO_{12} are 574.5 and 550.7 J K^{-1} mol^{-1}, respectively.

$$S^0_{298}(RE_6UO_{12}) = 3\,S^0_{298}(RE_2O_3) + S^0_{298}(UO_3)\ (RE = Gd,\ Nd)$$

Thermal expansion of Gd_6UO_{12} and Eu_6UO_{12}

The lattice parameters of Gd_6UO_{12} and Eu_6UO_{12} were estimated using NBSAIDS83 software. The diffraction pattern of the compounds could be indexed on $R\bar{3}$ space group as reported by Hinatsu et al. [2] and Jena et al. [5, 6]. The structural refinement of the samples was carried out by using the structure of iso-structural compounds La_6UO_{12} reported by Hinatsu et al. [2]. All reflections were indexed based on hexagonal crystallographic axes; for the Miller indices, the relationship $-h + k + l = 3n$ was observable. The lattice constants were found to expand along a and c axis. The thermal expansion measurements of the samples are presented up to 873 K to compare the effect of it on the heat capacity values of the compounds in the same temperature range. The percentage variation along the c-axis is observed to be comparatively lower than the a-axis. Similar observation was reported in our previous work [5] for RE_6UO_{12} (RE = La, Nd and Sm). The observed expansion behaviour can be explained based on crystal structure and bonding of the compounds. The chemical bonding in these compounds can be considered to be ionic in nature. In Gd_6UO_{12}, six oxygen atoms surround a uranium ion forming a distorted octahedron. Similarly, six oxygen atoms surround the Gd^{3+} ion in a highly distorted octahedral fashion. Hence both Gd and U are in six coordination sphere in Gd_6UO_{12}.The corners of UO_6 octahedra are shared by GdO_6 octahedra. Two edge shared GdO_6 octahedra separate two UO_6 along c-axis; this gives rigidity along the c-axis and therefore lowers percentage expansion with temperature. The lattice constants vs. T (K) of Gd_6UO_{12} and Eu_6UO_{12} are given in Fig. 4. The thermal expansions of the compounds showed an increasing trend with increasing temperature. The lattice constants of Eu_6UO_{12} are higher than Gd_6UO_{12} exhibiting the trend of lanthanide contraction. The coefficient of thermal expansion measured for Eu_6UO_{12} and Gd_6UO_{12} are shown in Table 4. The trends in the percentage variation along a and c axis for RE_6UO_{12} computed from the present investigation as well as from our previous study [5, 6] are given in Figs. 5 and 6, respectively. The trends in the variation of

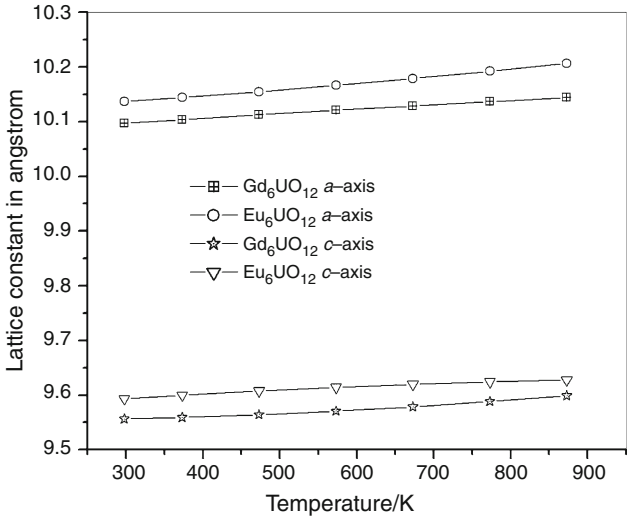

Fig. 4 Lattice expansion along *a*- and *c*-axis of Gd_6UO_{12} and Eu_6UO_{12}

Table 4 The average linear expansion coefficient along the hexagonal axes in the temperature range 298–873 K for RE_6UO_{12} compounds

Compounds	$\alpha_a/10^6\ K^{-1}$	$\alpha_c/10^6\ K^{-1}$
Eu_6UO_{12}	10.5 ± 1.0	7.3 ± 1.0
Gd_6UO_{12}	10.0 ± 1.0	9.7 ± 1.0
Gd_6UO_{12} [17]	9.6 ± 1.2	12.3 ± 3.6

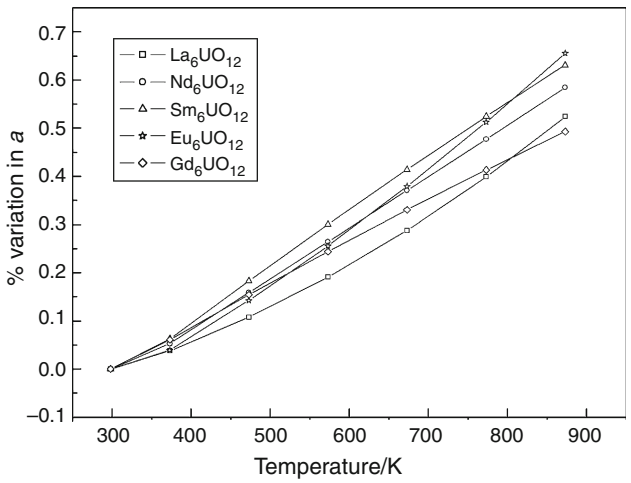

Fig. 5 Trend in % variation along *a*-axis with temperature for RE_6UO_{12}

percentage volume thermal expansion computed for RE_6UO_{12} from the present investigation as well as from our previous study [5, 6] are shown in Fig. 7. As can be seen in the Fig. 7, the percentage volume thermal expansion for RE_6UO_{12} varies as RE = Sm > Nd > Eu > La ≈ Gd.

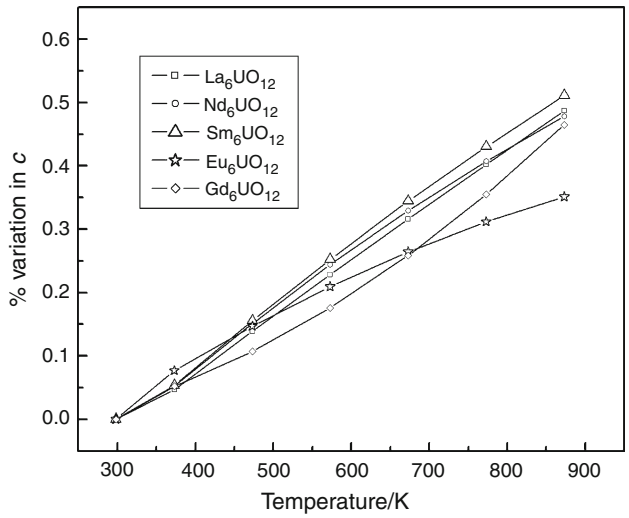

Fig. 6 Trend in % variation along *c*-axis with temperature for RE_6UO_{12}

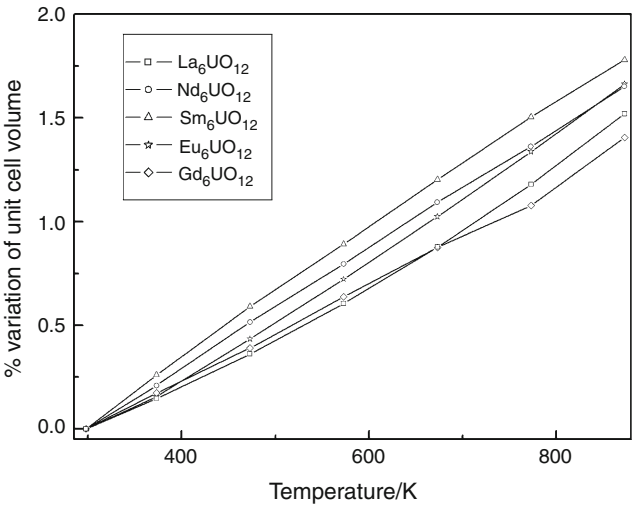

Fig. 7 Variation of percentage volume expansion of RE_6UO_{12} with temperature

Discussion

Heat capacity data of RE_6UO_{12} (RE = Nd, Gd) are compared with that for RE = La, Sm and Eu measured in our previous study [8] in Fig. 8. As can be seen in the Fig. 8, the heat capacity of RE_6UO_{12} varies in the order Eu_6UO_{12} [8] > Sm_6UO_{12} [8] > Nd_6UO_{12} > Gd_6UO_{12} > La_6UO_{12} [18]. Heat capacity of rare earth compounds includes contribution due to (1) phonons arising due to harmonic lattice vibration, (2) dilatational term arising due to thermal expansion and (3) Schottky contribution arising due to promotion of electrons to higher energy levels [24, 25]. As per theoretical expectations the contribution of phonons to heat capacity vary in RE_6UO_{12} as $La^{3+} > Nd^{3+} >$

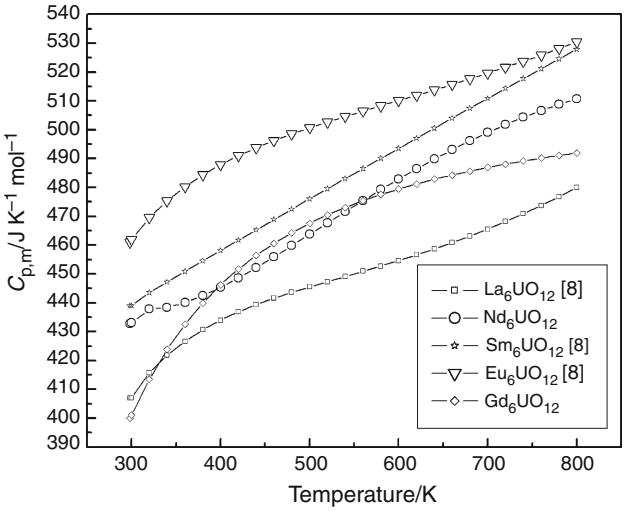

Fig. 8 Comparison of measured heat capacity data of RE_6UO_{12} vs. temperature

$Sm^{3+} > Eu^{3+} > Gd^{3+}$ as higher the size of the ions, phonon frequencies are expected to be lower and therefore higher will be the heat capacity. From the Fig. 7, it is evident that the contribution of thermal expansion to heat capacity of RE_6UO_{12} vary as $Sm^{3+} > Nd^{3+} > Eu^{3+} > La^{3+} \approx Gd^{3+}$. Though variation in the Schottky contribution to heat capacity for RE_6UO_{12} is difficult to predict, it is expected that it should be least in the case of La^{3+} (No 4f electrons) and lesser in the case of Gd^{3+} (half filled 4f shell) than Nd^{3+}, Eu^{3+} and Sm^{3+}. The observed trend in the variation of heat capacity of RE_6UO_{12} with varying RE could be due to the combined effect of all the three contributions to heat capacity mentioned above. The trend in the variation of heat capacity of RE_2O_3 as per the literature [23] is Gd < La < Nd < Sm < Eu. Whereas as per the present data the trend in the variation of heat capacity of RE_6UO_{12} is same as that of RE_2O_3 except for that of La and Gd. Sahu et al.[24] measured the heat capacity of Gd_6UO_{12} and compared with heat capacity data of RE_6UO_{12} (RE = La, Sm and Eu) from our previous work [18] and observed that trend in the variation of heat capacity of RE_6UO_{12} is same as the trend observed in that of RE_2O_3. It has to be noted that in the case of RE_2O_3, RE = La and Nd exhibits hexagonal structure [26] where as that of RE = Sm, Eu and Gd exhibits in both monoclinic and cubic form [26]. In the case of RE_6UO_{12}, all the compounds with RE = La to Gd exhibits rhombohedral structure. Therefore, trend in the variation in the heat capacity of RE_6UO_{12} need not follow that of RE_2O_3.

In our previous study [18] on the thermal expansion of RE_6UO_{12}, we could see an increasing trend in the % thermal expansion from the La through Nd to Sm compounds at any temperature. In the present study, we do not see the trend continuing to the Eu and Gd compounds. Thermal expansion of Eu_6UO_{12} and Gd_6UO_{12} falls within the range of that of the La, Nd and Sm systems as shown in Figs. 5, 6 and 7. This could be a manifestation of the peculiarity of the electronic configuration of the Eu and Gd ions. Gd^{3+} is $4f^7$ (half filled 4f level) and a part of Eu could be in $4f^7$, at high temperatures as result of the stability of Eu^{2+} state formed on loss of oxygen in Eu_6UO_{12}[1].

From Figs. 5 and 6 it could be observed that there is a slight increase in the slope of the % expansion along the *a* axis vs. *T* plot and a slight decrease in slope of the % expansion along the *c* axis vs. T plot for Eu_6UO_{12} at temperatures above 650 K. This is probably due to loss of oxygen from EuO_6 octahedra of Eu_6UO_{12} at high temperatures and consequent stabilization of Eu^{2+}. Similar observation was reported by Berndt et al. [1].

Conclusions

Heat capacity of Nd_6UO_{12} and Gd_6UO_{12} and thermal expansion coefficient of Eu_6UO_{12} and Gd_6UO_{12} were measured by DSC and HTXRD, respectively. The heat capacity of RE_6UO_{12} varies in the order $Eu_6UO_{12} > Sm_6UO_{12} > Nd_6UO_{12} > Gd_6UO_{12} > La_6UO_{12}$. The trend is explained on the basis of the contributions of different factors namely phonons arising due to harmonic vibration, thermal expansion arising due to unharmonic vibration and Schottky effect due to excitation of electrons to higher energy levels. Though increasing trend in the % thermal expansion was observed for RE_6UO_{12} for RE = La through Nd to Sm, the same is not maintained for Eu and Gd. Thermal expansion of RE_6UO_{12} (RE = Eu and Gd) falls within the range of that of the La, Nd and Sm systems. This may be due to the stable electronic configuration $4f^7$ for Gd^{3+} and Eu^{2+} (formed partly due to loss of oxygen in Eu_6UO_{12}.

References

1. Berndt U, Tanamas R, Keller C. The ternary UO2–UO3–EuO1.5 (EuO) system and investigation of Eu(II)-actinide(IV)-perovskites. J Solid State Chem. 1976;17:113–20.
2. Hinatsu Y, Masaki N, Fujino T. The crystal structure of La_6UO_{12}. J Solid State Chem. 1988;73:567–71.
3. Aitken EA, Bartram SF, Juenke EF. Crystal chemistry of the rhombohedral $MO_3{\cdot}3R_2O_3$ compounds. Inorg Chem. 1964;3:949–54.
4. Diehl HG, Keller C. Das system UO2–UO3–LaO1.5. J Solid State Chem. 1971;3:621–36.
5. Jena H, Asuvathraman R, Govindan Kutty KV. "Combustion synthesis and thermal expansion measurements of the rare earth–uranium ternary oxides RE_6UO_{12} (RE = La, Nd and Sm)". J Nucl Mater. 2000;280:312–7.
6. Jena H, Asuvathraman R, Krishnaiah MV, Govindan Kutty KV. X-ray powder diffraction of RE_6UO_{12} (RE = Eu, Gd and Dy). Powder Diffract. 2001;16(4):220–3.

7. Krishnaiah MV, Seenivasan G, Srirama Murti P, Mathews CK. Thermal conductivity of rare earth–uranium ternary oxides of the type RE6UO12. J Nucl Mater. 2002;306:10–4.
8. Panneerselvam G, Venkata Krishnan R, Nagarajan K, Antony MP. Thermal expansion and heat capacity of dysprosium hafnate. J Therm Anal Calorim. 2009 (in press).
9. Jagadeeswara Rao Ch, Venkata Krishnan R, Venkatesan KA, Nagarajan K, Srinivasan TG. Thermochemical properties of some bis(trifluoromethylsulfonyl)imide based room temperature ionic liquids. J Therm Anal Calorim. 2009;97:937–43.
10. Schick C. Differential scanning calorimetry (DSC) of semicrystalline polymers. Anal Bioanal Chem. 2009;395:1589–611.
11. Yoshida T, Moriya Y, Tojo T, Kawaji H, Atake T, Kuroiwa Y. Heat capacity at constant pressure and thermodynamic properties of phase transitions in $PbMO_3$ (M = Ti, Zr and Hf). J Therm Anal Calorim. 2009;95(2):675–83.
12. Lv X-C, Tan Z-C, Gao X-H, Shi Q, Sun L-X. Molar heat capacity and thermodynamic properties of crystalline $[Nd(Glu)(H_2O)(Im)_3](ClO_6)\cdot 2H_2O$. J Therm Anal Calorim. 2009;95(2):387–92.
13. Leitner J, Ruzicka K, Sedmidubsky D, Svoboda P. Heat capacity, enthalpy and entropy of calcium niobates. J Therm Anal Calorim. 2009;95(2):397–402.
14. Liu BP, Lv XC, Tan ZC, Zhang ZH, Shi Q, Yang LN, et al. Molar heat capacity and thermodynamic properties of crystalline $Ho(Asp)Cl_2\cdot 6H_2O$. J Therm Anal Calorim. 2007;89(1):283–7.
15. Tomaszkiewicz IZ, Swierzewski R, Gierycz P. Heat capacity of indium nitride. J Therm Anal Calorim. 2008;91(2):649–53.
16. Tomaszkiewicz IZ, Utzig E, Gierycz P. Heat capacity of crystalline GaN. J Therm Anal Calorim. 2008;91(1):329–32.
17. Arita Y, Ogawa T, Tsuchiya B, Matsui T. Heat capacity measurement and DSC study of hafnium hydrides. J Therm Anal Calorim. 2008;92(2):403–6.
18. Venkata Krishnan R, Manikandan P, Jena Hrudananda, Nagarajan K. Heat capacity of La_6UO_{12}, Sm_6UO_{12} and Eu_6UO_{12} by DSC. Thermochim Acta. 2008;472:95–8.
19. Venkata Krishnan R, Nagarajan K. Heat capacity measurements on uranium-cerium mixed oxides by differential scanning calorimetry. Thermochim Acta. 2006;440:141–5.
20. Venkata Krishnan R, Jena H, Govindan Kutty KV, Nagarajan K. Heat capacity of $Sr_{10}(PO_4)_6Cl_2$ and $Ca_{10}(PO_4)_6Cl_2$ by DSC. Thermochim Acta. 2008;478(1–2):13–6.
21. Venkata Krishnan R, Nagarajan K, Vasudeva Rao PR. Heat capacity measurements on $BaThO_3$ and $BaCeO_3$. J Nucl Mater. 2001;299:28–31.
22. Rand MH, Kubaschewski O. The thermochemical properties of uranium compounds. Edinburgh: Oliver and Boyd; 1963.
23. Pankratz LB. Thermodynamic properties of elements and oxides. Bull. US. Bur. Mines, 1982.
24. Sahu M, Krishnan K, Saxena MK, Ramkumar KL. Thermal expansion and Heat Capacity of Gd_6UO_{12}. J Alloys Compd. 2009;482(1–2):141–6.
25. Westrum EF Jr. Thermal and electronic properties of rare earth oxides. In: Kleber EV, editor. Rare earth research. New York: Macmillan Company; 1961. p. 69–80.
26. Zinkevich M. Thermodynamics of rare earth sesquioxides. Prog Mater Sci. 2007;52:597–647.